# Feedback Systems

*An Introduction for Scientists and Engineers*
*SECOND EDITION*

Karl Johan Åström
Richard M. Murray

Version v3.0c (10 January 2014)

This is the electronic edition of *Feedback Systems* and is available from http://www.cds.caltech.edu/~murray/amwiki. Hardcover editions may be purchased from Princeton Univeristy Press, http://press.princeton.edu/titles/8701.html.



PRINCETON UNIVERSITY PRESS
PRINCETON AND OXFORD

# Chapter Eleven
## Frequency Domain Design

*Sensitivity improvements in one frequency range must be paid for with sensitivity deteriorations in another frequency range, and the price is higher if the plant is open-loop unstable. This applies to every controller, no matter how it was designed.*

Gunter Stein in the inaugural IEEE Bode Lecture, 1989 [Ste03].

In this chapter we continue to explore the use of frequency domain techniques with a focus on the design of feedback systems. We begin with a more thorough description of the performance specifications for control systems and then introduce the concept of "loop shaping" as a mechanism for designing controllers in the frequency domain. We also introduce some fundamental limitations to performance for systems with time delays and right half-plane poles and zeros.

### 11.1 Sensitivity Functions

In the previous chapter, we considered the use of proportional-integral-derivative (PID) feedback as a mechanism for designing a feedback controller for a given process. In this chapter we will expand our approach to include a richer repertoire of tools for shaping the frequency response of the closed loop system.

One of the key ideas in this chapter is that we can design the behavior of the closed loop system by focusing on the open loop transfer function. This same approach was used in studying stability using the Nyquist criterion: we plotted the Nyquist plot for the *open* loop transfer function to determine the stability of the *closed* loop system. From a design perspective, the use of loop analysis tools is very powerful: since the loop transfer function is $L = PC$, if we can specify the desired performance in terms of properties of $L$, we can directly see the impact of changes in the controller $C$. This is much easier, for example, than trying to reason directly about the tracking response of the closed loop system, whose transfer function is given by $G_{yr} = PC/(1+PC)$.

We will start by investigating some key properties of the feedback loop. A block diagram of a basic feedback loop is shown in Figure 11.1. The system loop is composed of two components: the process and the controller. The controller itself has two blocks: the feedback block $C$ and the feedforward block $F$. There are two disturbances acting on the process, the load disturbance $v$ and the measurement noise $w$. The load disturbance represents disturbances that drive the process away from its desired behavior, while the measurement noise represents disturbances that corrupt information about the process given by the sensors. In the figure, the

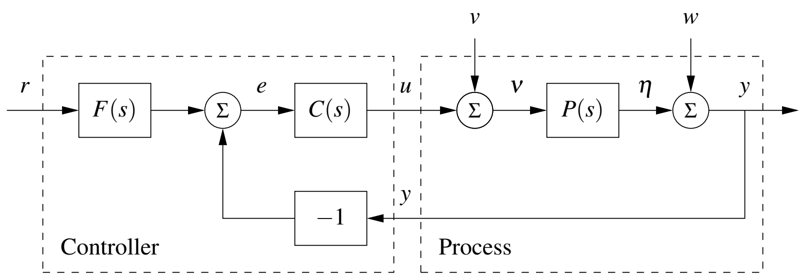


**Figure 11.1:** Block diagram of a basic feedback loop with two degrees of freedom. The controller has a feedback block $C$ and a feedforward block $F$. The external signals are the reference signal $r$, the load disturbance $v$ and the measurement noise $w$. The process output is $\eta$, and the control signal is $u$.

load disturbance is assumed to act on the process input. This is a simplification since disturbances often enter the process in many different ways, but it allows us to streamline the presentation without significant loss of generality.

The process output $\eta$ is the real variable that we want to control. Control is based on the measured signal $y$, where the measurements are corrupted by measurement noise $w$. The process is influenced by the controller via the control variable $u$. The process is thus a system with three inputs—the control variable $u$, the load disturbance $v$ and the measurement noise $w$—and one output—the measured signal $y$. The controller is a system with two inputs and one output. The inputs are the measured signal $y$ and the reference signal $r$, and the output is the control signal $u$. Note that the control signal $u$ is an input to the process and the output of the controller, and that the measured signal $y$ is the output of the process and an input to the controller.

The feedback loop in Figure 11.1 is influenced by three external signals, the reference $r$, the load disturbance $v$ and the measurement noise $w$. Any of the remaining signals can be of interest in controller design, depending on the particular application. Since the system is linear, the relations between the inputs and the interesting signals can be expressed in terms of the transfer functions. The following relations are obtained from the block diagram in Figure 11.1:

$$\begin{pmatrix} y \\ \eta \\ \nu \\ u \\ e \end{pmatrix} = \begin{pmatrix} \frac{PCF}{1+PC} & \frac{P}{1+PC} & \frac{1}{1+PC} \\ \frac{PCF}{1+PC} & \frac{P}{1+PC} & \frac{-PC}{1+PC} \\ \frac{CF}{1+PC} & \frac{1}{1+PC} & \frac{-C}{1+PC} \\ \frac{CF}{1+PC} & \frac{-PC}{1+PC} & \frac{-C}{1+PC} \\ \frac{F}{1+PC} & \frac{-P}{1+PC} & \frac{-1}{1+PC} \end{pmatrix} \begin{pmatrix} r \\ v \\ w \end{pmatrix}. \tag{11.1}$$

In addition, we can write the transfer function for the error between the reference

$r$ and the output $\eta$ (not an explicit signal in the diagram), which satisfies

$$\varepsilon = r - \eta = \Big(1 - \frac{PCF}{1+PC}\Big) r + \frac{-P}{1+PC} v + \frac{PC}{1+PC} w.$$

There are several interesting conclusions we can draw from these equations. First we can observe that several transfer functions are the same and that the majority of the relations are given by the following set of six transfer functions, which we call the *Gang of Six*:

$$\begin{aligned} TF &= \frac{PCF}{1+PC}, & T &= \frac{PC}{1+PC}, & PS &= \frac{P}{1+PC}, \\ CFS &= \frac{CF}{1+PC}, & CS &= \frac{C}{1+PC}, & S &= \frac{1}{1+PC}. \end{aligned} \tag{11.2}$$

The transfer functions in the first column give the response of the process output and control signal to the reference signal. The second column gives the response of the control variable to the load disturbance and the noise, and the final column gives the response of the process output to those two inputs. Notice that only four transfer functions are required to describe how the system reacts to load disturbances and measurement noise, and that two additional transfer functions are required to describe how the system responds to reference signals.

The linear behavior of the system is determined by the six transfer functions in equation (11.2), and specifications can be expressed in terms of these transfer functions. The special case when $F = 1$ is called a system with (pure) error feedback. In this case all control actions are based on feedback from the error only and the system is completely characterized by four transfer functions, namely, the four rightmost transfer functions in equation (11.2), which have specific names:

$$\begin{aligned} S &= \frac{1}{1+PC} \quad \text{sensitivity function} & PS &= \frac{P}{1+PC} \quad \text{load sensitivity function} \\ T &= \frac{PC}{1+PC} \quad \text{complementary sensitivity function} & CS &= \frac{C}{1+PC} \quad \text{noise sensitivity function} \end{aligned} \tag{11.3}$$

These transfer functions and their equivalent systems are called the *Gang of Four*. The load sensitivity function is sometimes called the input sensitivity function and the noise sensitivity function is sometimes called the output sensitivity function. These transfer functions have many interesting properties that will be discussed in detail in the rest of the chapter. Good insight into these properties is essential in understanding the performance of feedback systems for the purposes of both analysis and design.

Analyzing the Gang of Six, we find that the feedback controller $C$ influences the effects of load disturbances and measurement noise. Notice that measurement noise enters the process via the feedback. In Section 12.2 it will be shown that the controller influences the sensitivity of the closed loop to process variations.

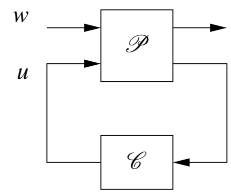


**Figure 11.2:** A more general representation of a feedback system. The process input $u$ represents the control signal, which can be manipulated, and the process input $w$ represents other signals that influence the process. The process output $y$ is the vector of measured variables and $z$ are other signals of interest.

The feedforward part $F$ of the controller influences only the response to command signals.

In Chapter 9 we focused on the loop transfer function, and we found that its properties gave useful insights into the properties of a system. To make a proper assessment of a feedback system it is necessary to consider the properties of all the transfer functions (11.2) in the Gang of Six or the Gang of Four, as illustrated in the following example.

**Example 11.1 The loop transfer function gives only limited insight**
Consider a process with the transfer function $P(s) = 1/(s-a)$ controlled by a PI controller with error feedback having the transfer function $C(s) = k(s-a)/s$. The loop transfer function is $L = k/s$, and the sensitivity functions are

$$T = \frac{PC}{1+PC} = \frac{k}{s+k}, \qquad PS = \frac{P}{1+PC} = \frac{s}{(s-a)(s+k)},$$
$$CS = \frac{C}{1+PC} = \frac{k(s-a)}{s+k}, \qquad S = \frac{1}{1+PC} = \frac{s}{s+k}.$$

Notice that the factor $s-a$ is canceled when computing the loop transfer function and that this factor also does not appear in the sensitivity function or the complementary sensitivity function. However, cancellation of the factor is very serious if $a > 0$ since the transfer function $PS$ relating load disturbances to process output is then unstable. In particular, a small disturbance $v$ can lead to an unbounded output, which is clearly not desirable. ∇

The system in Figure 11.1 represents a special case because it is assumed that the load disturbance enters at the process input and that the measured output is the sum of the process variable and the measurement noise. Disturbances can enter in many different ways, and the sensors may have dynamics. A more abstract way to capture the general case is shown in Figure 11.2, which has only two blocks representing the process ($\mathscr{P}$) and the controller ($\mathscr{C}$). The process has two inputs, the control signal $u$ and a vector of disturbances $w$, and two outputs, the measured signal $y$ and a vector of signals $z$ that is used to specify performance. If we omit the reference input $r$, the system in Figure 11.1 can be captured by choosing $w = (d, n)$ and $z = (\eta, \nu, e, \varepsilon)$. The process transfer function $\mathscr{P}$ is a $5 \times 3$ matrix, and the controller transfer function $\mathscr{C}$ is a $1 \times 1$ matrix; compare with Exercise 11.3.

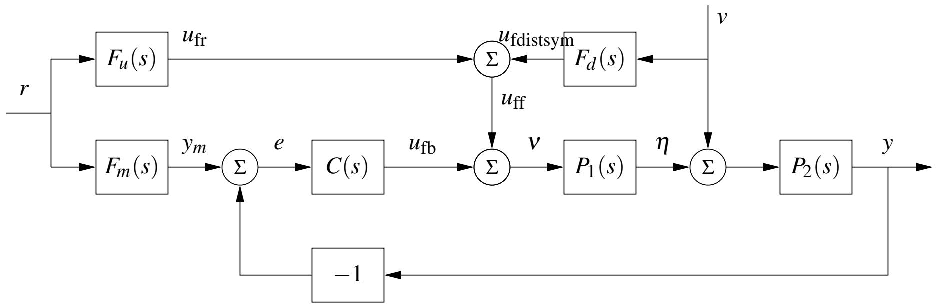


**Figure 11.3:** Block diagram of a system with feedforward compensation for improved response to reference signals and measured disturbances (2 DOF system). Three feedforward elements are present: $F_m(s)$ sets the desired output value, $F_u(s)$ generates the feedforward command $u_{fr}$ and $F_d(s)$ attempts to cancel disturbances.

Processes with multiple inputs and outputs can also be considered by regarding $u$ and $y$ as vectors. Representations at these higher levels of abstraction are useful for the development of theory because they make it possible to focus on fundamentals and to solve general problems with a wide range of applications. However, care must be exercised to maintain the coupling to the real-world control problems we intend to solve.

## 11.2 Feedforward Design

Most of our analysis and design tools up to this point have focused on the role of feedback and its effect on the dynamics of the system. Feedforward is a simple and powerful technique that complements feedback. It can be used both to improve the response to reference signals and to reduce the effect of measurable disturbances. Feedforward compensation admits perfect elimination of disturbances, but it is much more sensitive to process variations than feedback compensation. A general scheme for feedforward was discussed in Section 7.5 using Figure 7.10. A simple form of feedforward for PID controllers was discussed in Section 10.5. The controller in Figure 11.1 also has a feedforward block to improve response to command signals. An alternative version of feedforward is shown in Figure 11.3, which we will use in this section to understand some of the trade-offs between feedforward and feedback.

Controllers with two degrees of freedom (feedforward and feedback) have the advantage that the response to reference signals can be designed independently of the design for disturbance attenuation and robustness. We will first consider the response to reference signals, and we will therefore initially assume that the load disturbance $v$ is zero. Let $F_m$ represent the ideal response of the system to reference signals. The feedforward compensator is characterized by the transfer functions $F_u$ and $F_m$. When the reference is changed, the transfer function $F_u$ generates the signal $u_{fr}$, which is chosen to give the desired output when applied as input to the process. Under ideal conditions the output $y$ is then equal to $y_m$, the error signal is zero and there will be no feedback action. If there are disturbances or modeling errors, the signals $y_m$ and $y$ will differ. The feedback then attempts to bring the error to zero.

To make a formal analysis, we compute the transfer function from reference input to process output:

$$G_{yr}(s) = \frac{P(CF_m + F_u)}{1 + PC} = F_m + \frac{PF_u - F_m}{1 + PC}, \tag{11.4}$$

where $P = P_2 P_1$. The first term represents the desired transfer function. The second term can be made small in two ways. Feedforward compensation can be used to make $PF_u - F_m$ small, or feedback compensation can be used to make $1 + PC$ large. Perfect feedforward compensation is obtained by choosing

$$F_u = \frac{F_m}{P}. \tag{11.5}$$

Design of feedforward using transfer functions is thus a very simple task. Notice that the feedforward compensator $F_u$ contains an inverse model of the process dynamics.

Feedback and feedforward have different properties. Feedforward action is obtained by matching two transfer functions, requiring precise knowledge of the process dynamics, while feedback attempts to make the error small by dividing it by a large quantity. For a controller having integral action, the loop gain is large for low frequencies, and it is thus sufficient to make sure that the condition for ideal feedforward holds at higher frequencies. This is easier than trying to satisfy the condition (11.5) for all frequencies.

We will now consider reduction of the effects of the load disturbance $v$ in Figure 11.3 by feedforward control. We assume that the disturbance signal is measured and that the disturbance enters the process dynamics in a known way (captured by $P_1$ and $P_2$). The effect of the disturbance can be reduced by feeding the measured signal through a dynamical system with the transfer function $F_d$. Assuming that the reference $r$ is zero, we can use block diagram algebra to find that the transfer function from the disturbance to the process output is

$$G_{yv} = \frac{P_2(1 + P_1 F_d)}{1 + PC}, \tag{11.6}$$

where $P = P_2 P_1$. The effect of the disturbance can be reduced by making $1 + F_d P_1$ small (feedforward) or by making $1 + PC$ large (feedback). Perfect compensation is obtained by choosing

$$F_d = -P_1^{-1}, \tag{11.7}$$

requiring inversion of the transfer function $P_1$.

As in the case of reference tracking, disturbance attenuation can be accomplished by combining feedback and feedforward control. Since low-frequency disturbances can be eliminated by feedback, we require the use of feedforward only for high-frequency disturbances, and the transfer function $F_d$ in equation (11.7) can then be computed using an approximation of $P_1$ for high frequencies.

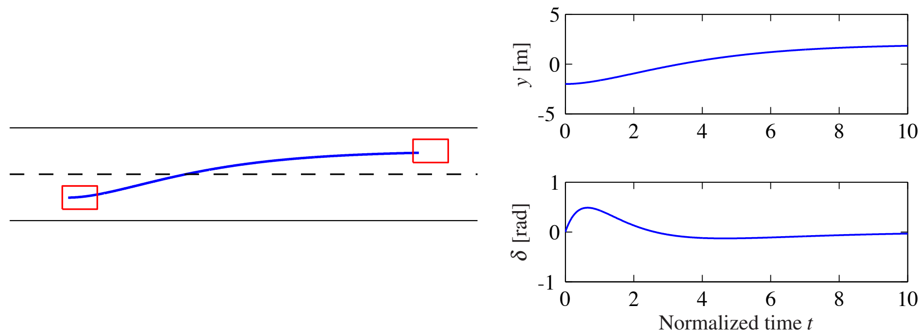


(a) Overhead view

(b) Position and steering

**Figure 11.4:** Feedforward control for vehicle steering. The plot on the left shows the trajectory generated by the controller for changing lanes. The plots on the right show the lateral deviation $y$ (top) and the steering angle $\delta$ (bottom) for a smooth lane change control using feedforward (based on the linearized model).

Equations (11.5) and (11.7) give analytic expressions for the feedforward compensator. To obtain a transfer function that can be implemented without difficulties we require that the feedforward compensator be stable and that it does not require differentiation. Therefore there may be constraints on possible choices of the desired response $F_m$, and approximations are needed if the process has zeros in the right half-plane or time delays.

**Example 11.2 Vehicle steering**

A linearized model for vehicle steering was given in Example 6.4. The normalized transfer function from steering angle $\delta$ to lateral deviation $y$ is $P(s) = (\gamma s + 1)/s^2$. For a lane transfer system we would like to have a nice response without overshoot, and we therefore choose the desired response as $F_m(s) = a^2/(s+a)^2$, where the response speed or aggressiveness of the steering is governed by the parameter $a$. Equation (11.5) gives

$$F_u = \frac{F_m}{P} = \frac{a^2 s^2}{(\gamma s + 1)(s+a)^2},$$

which is a stable transfer function as long as $\gamma > 0$. Figure 11.4 shows the responses of the system for $a = 0.5$. The figure shows that a lane change is accomplished in about 10 vehicle lengths with smooth steering angles. The largest steering angle is slightly larger than 0.1 rad (6°). Using the scaled variables, the curve showing lateral deviations ($y$ as a function of $t$) can also be interpreted as the vehicle path ($y$ as a function of $x$) with the vehicle length as the length unit. ∇

A major advantage of controllers with two degrees of freedom that combine feedback and feedforward is that the control design problem can be split in two parts. The feedback controller $C$ can be designed to give good robustness and effective disturbance attenuation, and the feedforward part can be designed independently to give the desired response to command signals.

## 11.3 Performance Specifications

A key element of the control design process is how we specify the desired performance of the system. It is also important for users to understand performance specifications so that they know what to ask for and how to test a system. Specifications are often given in terms of robustness to process variations and responses to reference signals and disturbances. They can be given in terms of both time and frequency responses. Specifications for the step response to reference signals were given in Figure 5.9 in Section 5.3 and in Section 6.3. Robustness specifications based on frequency domain concepts were provided in Section 9.3 and will be considered further in Chapter 12. The specifications discussed previously were based on the loop transfer function. Since we found in Section 11.1 that a single transfer function did not always characterize the properties of the closed loop completely, we will give a more complete discussion of specifications in this section, based on the full Gang of Six.

The transfer function gives a good characterization of the linear behavior of a system. To provide specifications it is desirable to capture the characteristic properties of a system with a few parameters. Common features for time responses are overshoot, rise time and settling time, as shown in Figure 5.9. Common features of frequency responses are resonant peak, peak frequency, gain crossover frequency and bandwidth. A *resonant peak* is a maximum of the gain, and the peak frequency is the corresponding frequency. The *gain crossover frequency* is the frequency where the open loop gain is equal one. The *bandwidth* is defined as the frequency range where the closed loop gain is $1/\sqrt{2}$ of the low-frequency gain (low-pass), mid-frequency gain (band-pass) or high-frequency gain (high-pass). There are interesting relations between specifications in the time and frequency domains. Roughly speaking, the behavior of time responses for short times is related to the behavior of frequency responses at high frequencies, and vice versa. The precise relations are not trivial to derive.

### Response to Reference Signals

Consider the basic feedback loop in Figure 11.1. The response to reference signals is described by the transfer functions $G_{yr} = PCF/(1+PC)$ and $G_{ur} = CF/(1+PC)$ ($F = 1$ for systems with error feedback). Notice that it is useful to consider both the response of the output and that of the control signal. In particular, the control signal response allows us to judge the magnitude and rate of the control signal required to obtain the output response.

**Example 11.3 Third-order system**
Consider a process with the transfer function $P(s) = (s+1)^{-3}$ and a PI controller with error feedback having the gains $k_p = 0.6$ and $k_i = 0.5$. The responses are illustrated in Figure 11.5. The solid lines show results for a proportional-integral (PI) controller with error feedback. The dashed lines show results for a controller with feedforward designed to give the transfer function $G_{yr} = (0.5s+1)^{-3}$. Looking at the time responses, we find that the controller with feedforward gives a faster

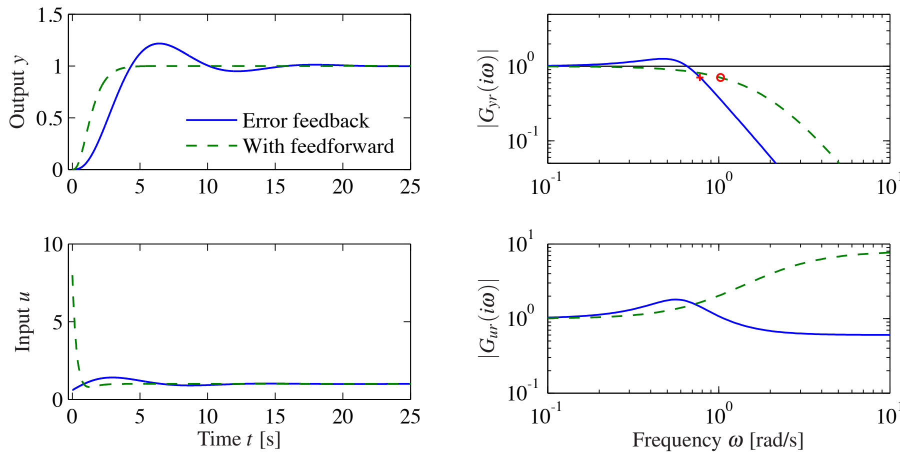


(a) Step responses (b) Frequency responses

**Figure 11.5:** Reference signal responses. The responses in process output $y$ and control signal $u$ to a unit step in the reference signal $r$ are shown in (a), and the gain curves of $G_{yr}$ and $G_{ur}$ are shown in (b). Results with PI control with error feedback are shown by solid lines, and the dashed lines show results for a controller with a feedforward compensator.

response with no overshoot. However, much larger control signals are required to obtain the fast response. The largest value of the control signal is 8, compared to 1.2 for the regular PI controller. The controller with feedforward has a larger bandwidth (marked with ◦) and no resonant peak. The transfer function $G_{ur}$ also has higher gain at high frequencies. ∇

### Response to Load Disturbances and Measurement Noise

A simple criterion for disturbance attenuation is to compare the output of the closed loop system in Figure 11.1 with the output of the corresponding open loop system obtained by setting $C = 0$. If we let the disturbances for the open and closed loop systems be identical, the output of the closed loop system is then obtained simply by passing the open loop output through a system with the transfer function $S$. The sensitivity function tells how the variations in the output are influenced by feedback (Exercise 11.7). Disturbances with frequencies such that $|S(i\omega)| < 1$ are attenuated, but disturbances with frequencies such that $|S(i\omega)| > 1$ are amplified by feedback. The maximum sensitivity $M_s$, which occurs at the frequency $\omega_{ms}$, is thus a measure of the largest amplification of the disturbances. The maximum magnitude of $1/(1+L)$ is also the minimum of $|1+L|$, which is precisely the stability margin $s_m$ defined in Section 9.3, so that $M_s = 1/s_m$. The maximum sensitivity is therefore also a robustness measure.

If the sensitivity function is known, the potential improvements by feedback can be evaluated simply by recording a typical output and filtering it through the sensitivity function. A plot of the gain curve of the sensitivity function is a good way to make an assessment of the disturbance attenuation. Since the sensitivity

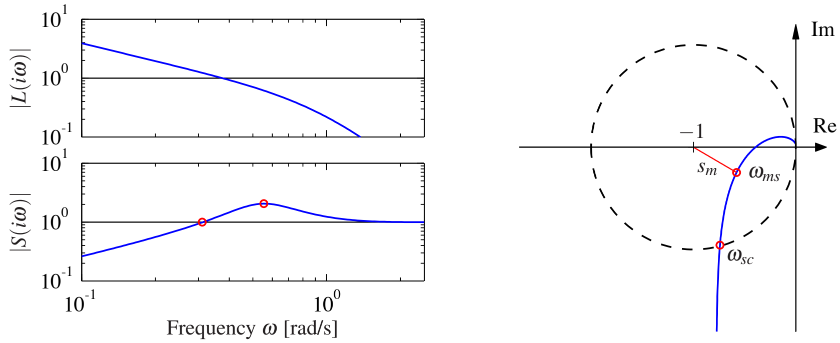


(a) Gain curves

(b) Nyquist plot

**Figure 11.6:** Graphical interpretation of the sensitivity function. Gain curves of the loop transfer function and the sensitivity function (a) can be used to calculate the properties of the sensitivity function through the relation $S = 1/(1+L)$. The sensitivity crossover frequency $\omega_{sc}$ and the frequency $\omega_{ms}$ where the sensitivity has its largest value are indicated in the sensitivity plot. The Nyquist plot (b) shows the same information in a different form. All points inside the dashed circle have sensitivities greater than 1.

function depends only on the loop transfer function, its properties can also be visualized graphically using the Nyquist plot of the loop transfer function. This is illustrated in Figure 11.6. The complex number $1 + L(i\omega)$ can be represented as the vector from the point $-1$ to the point $L(i\omega)$ on the Nyquist curve. The sensitivity is thus less than 1 for all points outside a circle with radius 1 and center at $-1$. Disturbances with frequencies in this range are attenuated by the feedback.

The transfer function $G_{yv}$ from load disturbance $v$ to process output $y$ for the system in Figure 11.1 is

$$G_{yv} = \frac{P}{1+PC} = PS = \frac{T}{C}. \tag{11.8}$$

Since load disturbances typically have low frequencies, it is natural to focus on the behavior of the transfer function at low frequencies. For a system with $P(0) \neq 0$ and a controller with integral action, the controller gain goes to infinity for small frequencies and we have the following approximation for small $s$:

$$G_{yv} = \frac{T}{C} \approx \frac{1}{C} \approx \frac{s}{k_i}, \tag{11.9}$$

where $k_i$ is the integral gain. Since the sensitivity function $S$ goes to 1 for large $s$, we have the approximation $G_{yv} \approx P$ for high frequencies.

Measurement noise, which typically has high frequencies, generates rapid variations in the control variable that are detrimental because they cause wear in many actuators and can even saturate an actuator. It is thus important to keep variations in the control signal due to measurement noise at reasonable levels—a typical requirement is that the variations are only a fraction of the span of the control signal. The variations can be influenced by filtering and by proper design of the high-

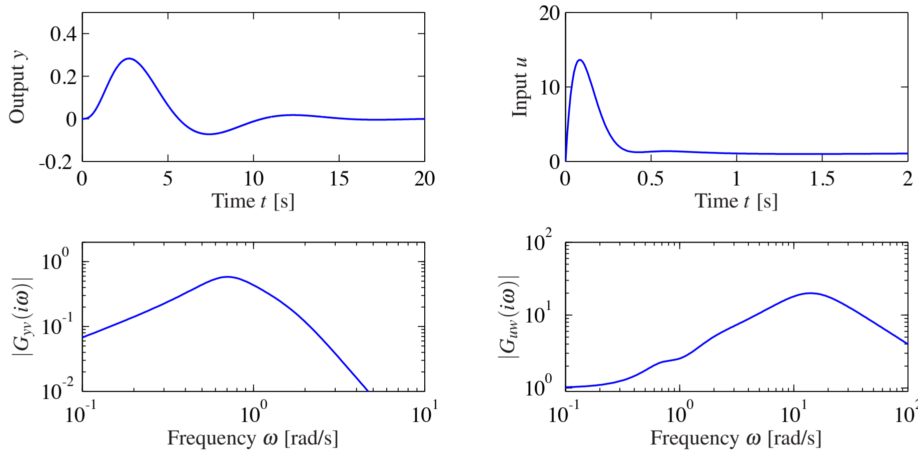


**Figure 11.7:** Disturbance responses. The time and frequency responses of process output $y$ to load disturbance $v$ are shown in (a) and the responses of control signal $u$ to measurement noise $w$ are shown in (b).

frequency properties of the controller.

The effects of measurement noise are captured by the transfer function from the measurement noise to the control signal,

$$-G_{uw} = \frac{C}{1+PC} = CS = \frac{T}{P}. \tag{11.10}$$

The complementary sensitivity function is close to 1 for low frequencies ($\omega < \omega_{\text{gc}}$), and $G_{uw}$ can be approximated by $-1/P$. The sensitivity function is close to 1 for high frequencies ($\omega > \omega_{\text{gc}}$), and $G_{uw}$ can be approximated by $-C$.

**Example 11.4 Third-order system**

Consider a process with the transfer function $P(s) = (s+1)^{-3}$ and a proportional-integral-derivative (PID) controller with gains $k_p = 0.6$, $k_i = 0.5$ and $k_d = 2.0$. We augment the controller using a second-order noise filter with $T_f = 0.1$, so that its transfer function is

$$C(s) = \frac{k_d s^2 + k_p s + k_i}{s(s^2 T_f^2/2 + sT_f + 1)}.$$

The system responses are illustrated in Figure 11.7. The response of the output to a step in the load disturbance in the top part of Figure 11.7a has a peak of 0.28 at time $t = 2.73$ s. The frequency response in Figure 11.7a shows that the gain has a maximum of 0.58 at $\omega = 0.7$ rad/s.

The response of the control signal to a step in measurement noise is shown in Figure 11.7b. The high-frequency roll-off of the transfer function $G_{uw}(i\omega)$ is due to filtering; without it the gain curve in Figure 11.7b would continue to rise after 20 rad/s. The step response has a peak of 13 at $t = 0.08$ s. The frequency response has its peak 20 at $\omega = 14$ rad/s. Notice that the peak occurs far above the peak

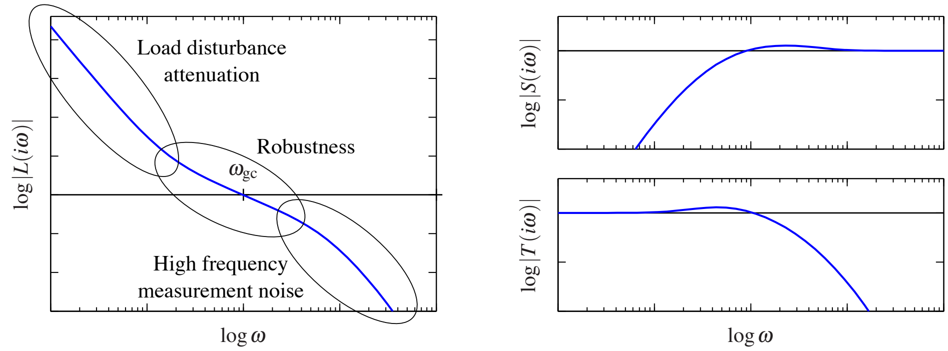


**Figure 11.8:** Gain curve and sensitivity functions for a typical loop transfer function. The plot on the left shows the gain curve and the plots on the right show the sensitivity function and complementary sensitivity function. The gain crossover frequency $\omega_{gc}$ and the slope $n_{gc}$ of the gain curve at crossover are important parameters that determine the robustness of closed loop systems. At low frequency, a large magnitude for $L$ provides good load disturbance rejection and reference tracking, while at high frequency a small loop gain is used to avoid amplifying measurement noise.

of the response to load disturbances and far above the gain crossover frequency $\omega_{gc} = 0.78$ rad/s. An approximation derived in Exercise 11.9 gives $\max|CS(i\omega)| \approx k_d/T_f = 20$, which occurs at $\omega = \sqrt{2}/T_d = 14.1$ rad/s. ∇

## 11.4 Feedback Design via Loop Shaping

One advantage of the Nyquist stability theorem is that it is based on the loop transfer function, which is related to the controller transfer function through $L = PC$. It is thus easy to see how the controller influences the loop transfer function. To make an unstable system stable we simply have to bend the Nyquist curve away from the critical point.

This simple idea is the basis of several different design methods collectively called *loop shaping*. These methods are based on choosing a compensator that gives a loop transfer function with a desired shape. One possibility is to determine a loop transfer function that gives a closed loop system with the desired properties and to compute the controller as $C = L/P$. Another is to start with the process transfer function, change its gain and then add poles and zeros until the desired shape is obtained. In this section we will explore different loop-shaping methods for control law design.

### Design Considerations

We will first discuss a suitable shape for the loop transfer function that gives good performance and good stability margins. Figure 11.8 shows a typical loop transfer function. Good robustness requires good stability margins (or good gain and phase margins), which imposes requirements on the loop transfer function around the crossover frequencies $\omega_{pc}$ and $\omega_{gc}$. The gain of $L$ at low frequencies must be large in order to have good tracking of command signals and good attenuation of low-frequency disturbances. Since $S = 1/(1+L)$, it follows that for frequencies where $|L| > 101$ disturbances will be attenuated by a factor of 100 and the tracking error is less than 1%. It is therefore desirable to have a large crossover frequency and a steep (negative) slope of the gain curve. The gain at low frequencies can be increased by a controller with integral action, which is also called *lag compensation*. To avoid injecting too much measurement noise into the system, the loop transfer function should have low gain at high frequencies, which is called *high-frequency roll-off*. The choice of gain crossover frequency is a compromise among attenuation of load disturbances, injection of measurement noise and robustness.

Bode's relations (see Section 9.4) impose restrictions on the shape of the loop transfer function. Equation (9.8) implies that the slope of the gain curve at gain crossover cannot be too steep. If the gain curve has a constant slope, we have the following relation between slope $n_{gc}$ and phase margin $\varphi_m$:

$$n_{gc} = -2 + \frac{2\varphi_m}{\pi}. \tag{11.11}$$

This formula is a reasonable approximation when the gain curve does not deviate too much from a straight line. It follows from equation (11.11) that the phase margins 30°, 45° and 60° correspond to the slopes $-5/3$, $-3/2$ and $-4/3$.

Loop shaping is a trial-and-error procedure. We typically start with a Bode plot of the process transfer function. We then attempt to shape the loop transfer function by changing the controller gain and adding poles and zeros to the controller transfer function. Different performance specifications are evaluated for each controller as we attempt to balance many different requirements by adjusting controller parameters and complexity. Loop shaping is straightforward to apply to single-input, single-output systems. It can also be applied to systems with one input and many outputs by closing the loops one at a time starting with the innermost loop. The only limitation for minimum phase systems is that large phase leads and high controller gains may be required to obtain closed loop systems with a fast response. Many specific procedures are available: they all require experience, but they also give good insight into the conflicting requirements. There are fundamental limitations to what can be achieved for systems that are not minimum phase; they will be discussed in the next section.

### Lead and Lag Compensation

A simple way to do loop shaping is to start with the transfer function of the process and add simple compensators with the transfer function

$$C(s) = k\frac{s+a}{s+b}. \tag{11.12}$$

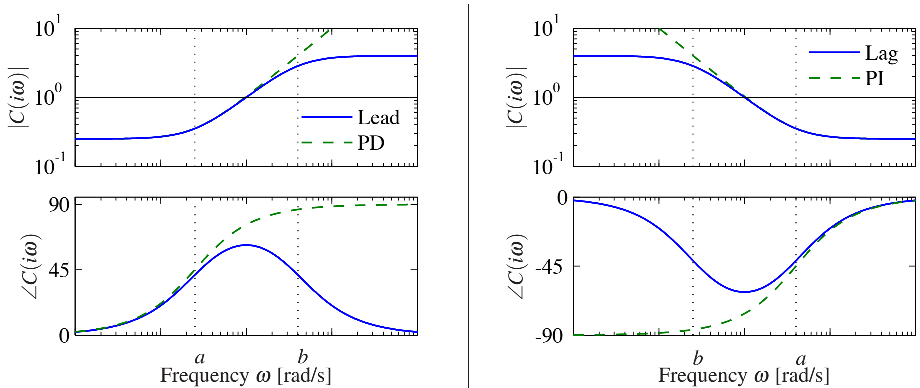


(a) Lead compensation, $a < b$

(b) Lag compensation, $b < a$

**Figure 11.9:** Frequency response for lead and lag compensators $C(s) = k(s+a)/(s+b)$. Lead compensation (a) occurs when $a < b$ and provides phase lead between $\omega = a$ and $\omega = b$. Lag compensation (b) corresponds to $a > b$ and provides low-frequency gain. PI control is a special case of lag compensation and PD control is a special case of lead compensation. PI/PD frequency responses are shown by dashed curves.

The compensator is called a *lead compensator* if $a < b$, and a *lag compensator* if $a > b$. The PI controller is a special case of a lag compensator with $b = 0$, and the ideal PD controller is a special case of a lead compensator with $a = 0$. Bode plots of lead and lag compensators are shown in Figure 11.9. Lag compensation, which increases the gain at low frequencies, is typically used to improve tracking performance and disturbance attenuation at low frequencies. Compensators that are tailored to specific disturbances can be also designed, as shown in Exercise 11.10. Lead compensation is typically used to improve phase margin. The following examples give illustrations.

**Example 11.5 Atomic force microscope in tapping mode**
A simple model of the dynamics of the vertical motion of an atomic force microscope in tapping mode was given in Exercise 9.2. The transfer function for the system dynamics is

$$P(s) = \frac{a(1-e^{-s\tau})}{s\tau(s+a)},$$

where $a = \zeta\omega_0$, $\tau = 2\pi n/\omega_0$ and the gain has been normalized to 1. A Bode plot of this transfer function for the parameters $a = 1$ and $\tau = 0.25$ is shown in dashed curves in Figure 11.10a. To improve the attenuation of load disturbances we increase the low-frequency gain by introducing an integral controller. The loop transfer function then becomes $L = k_i P(s)/s$, and we adjust the gain so that the phase margin is zero, giving $k_i = 8.3$. The Bode plot is shown by the dash-dotted line in Figure 11.10a, where the critical point is indicated by $\circ$. Notice the increase of the gain at low frequencies. To improve the phase margin we introduce proportional action and we increase the proportional gain $k_p$ gradually until reasonable values of the sensitivities are obtained. The value $k_p = 3.5$ gives maximum sensitivity

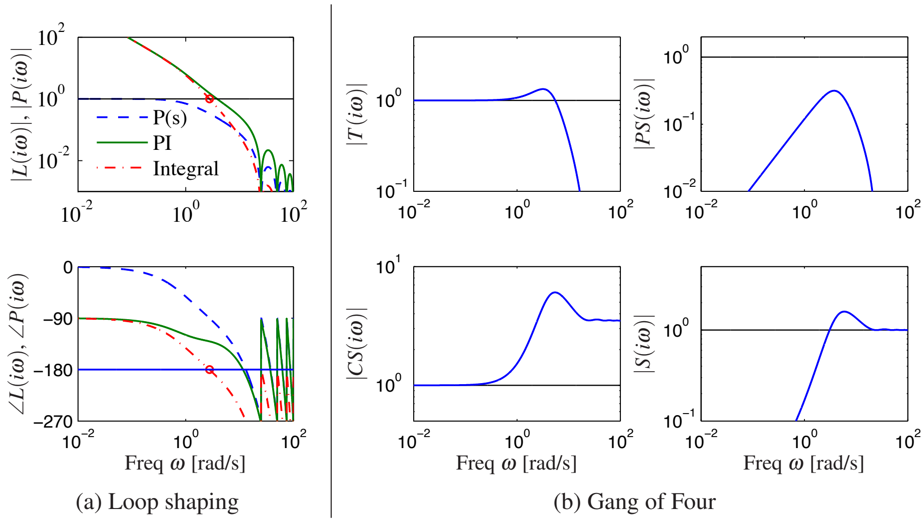


**Figure 11.10:** Loop-shaping design of a controller for an atomic force microscope in tapping mode. (a) Bode plots of the process (dashed), the loop transfer function for an integral controller with critical gain (dash-dotted) and a PI controller (solid) adjusted to give reasonable robustness. (b) Gain curves for the Gang of Four for the system.

$M_s = 1.6$ and maximum complementary sensitivity $M_t = 1.3$. The loop transfer function is shown in solid lines in Figure 11.10a. Notice the significant increase of the phase margin compared with the purely integral controller (dash-dotted line).

To evaluate the design we also compute the gain curves of the transfer functions in the Gang of Four. They are shown in Figure 11.10b. The peaks of the sensitivity curves are reasonable, and the plot of $PS$ shows that the largest value of $PS$ is 0.3, which implies that the load disturbances are well attenuated. The plot of $CS$ shows that the largest controller gain is 6. The controller has a gain of 3.5 at high frequencies, and hence we may consider adding high-frequency roll-off. ∇

A common problem in the design of feedback systems is that the phase margin is too small, and phase *lead* must then be added to the system. If we set $a < b$ in equation (11.12), we add phase lead in the frequency range between the pole/zero pair (and extending approximately $10\times$ in frequency in each direction). By appropriately choosing the location of this phase lead, we can provide additional phase margin at the gain crossover frequency.

Because the phase of a transfer function is related to the slope of the magnitude, increasing the phase requires increasing the gain of the loop transfer function over the frequency range in which the lead compensation is applied. In Exercise 11.13 it is shown that the gain increases exponentially with the amount of phase lead. We can also think of the lead compensator as changing the slope of the transfer function and thus shaping the loop transfer function in the crossover region (although it can be applied elsewhere as well).

**Example 11.6 Roll control for a vectored thrust aircraft**

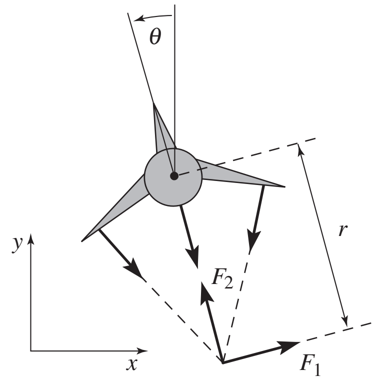


(a) Simplified model

| Symbol | Description | Value |
|---|---|---|
| $m$ | Vehicle mass | 4.0 kg |
| $J$ | Vehicle inertia, $\varphi_3$ axis | 0.0475 kg m$^2$ |
| $r$ | Force moment arm | 25.0 cm |
| $c$ | Damping coefficient | 0.05 kg m/s |
| $g$ | Gravitational constant | 9.8 m/s$^2$ |

(b) Parameter values

**Figure 11.11:** Roll control of a vectored thrust aircraft. (a) The roll angle $\theta$ is controlled by applying maneuvering thrusters, resulting in a moment generated by $F_1$. (b) The table lists the parameter values for a laboratory version of the system.

Consider the control of the roll of a vectored thrust aircraft such as the one illustrated in Figure 11.11. Following Exercise 8.10, we model the system with a second-order transfer function of the form

$$P(s) = \frac{r}{Js^2},$$

with the parameters given in Figure 11.11b. We take as our performance specification that we would like less than 1% error in steady state and less than 10% tracking error up to 10 rad/s.

The open loop transfer function is shown in Figure 11.12a. To achieve our performance specification, we would like to have a gain of at least 10 at a frequency of 10 rad/s, requiring the gain crossover frequency to be at a higher frequency. We see from the loop shape that in order to achieve the desired performance we cannot simply increase the gain since this would give a very low phase margin. Instead, we must increase the phase at the desired crossover frequency.

To accomplish this, we use a lead compensator (11.12) with $a = 2$ and $b = 50$. We then set the gain of the system to provide a large loop gain up to the desired bandwidth, as shown in Figure 11.12b. We see that this system has a gain of greater than 10 at all frequencies up to 10 rad/s and that it has more than 60° of phase margin. ∇

The action of a lead compensator is essentially the same as that of the derivative portion of a PID controller. As described in Section 10.5, we often use a filter for the derivative action of a PID controller to limit the high-frequency gain. This same effect is present in a lead compensator through the pole at $s = b$.

Equation (11.12) is a first-order compensator and can provide up to 90° of phase lead. Larger phase lead can be obtained by using a higher-order lead com-

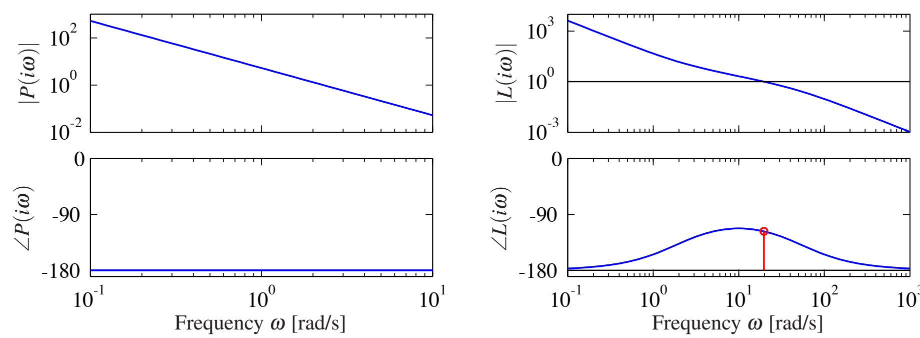


(a) Process dynamics

(b) Lead compensator

**Figure 11.12:** Control design for a vectored thrust aircraft using lead compensation. The Bode plot for the open loop process $P$ is shown in (a) and the loop transfer function $L = PC$ using a lead compensator in (b). Note the phase lead in the crossover region near $\omega = 100$ rad/s.

pensator (Exercise 11.13):

$$C(s) = k\frac{(s+a)^n}{(s+b)^n}, \qquad a < b.$$

## 11.5 The Root-Locus Method

In the design methods like pole placement in Sections 3.2, 3.3 and 7.3. we designed controllers that give desired closed loop poles. The controllers were sufficiently complex so that all closed loop poles could be specified. The complexity of the controller is thus related to the complexity of the process. In a practice we may have to use a simple controller for a complex process and it is then not possible to find a controller that gives all closed poles their desired values. It is interesting to explore what can be done with a controller having restricted complexity as was the case for loop shaping in Section 11.4. The simplest case with only one selectable controller parameter can be investigated with the *root locus method*. The *root locus* is a graph of the roots of the characteristic equation as a function of the parameter. The method gives insight into the effects of the controller parameter. It is straight forward to obtain the root locus by finding the roots of of the closed-loop characteristic polynomial for different values of the parameter. There are also good computer tools for generating the root locus. Of greater interest is that the general shape of the root locus can be obtained with very little effort.

### Proportional Control

To illustrate the root locus method we consider a process with the transfer function

$$P(s) = \frac{b(s)}{a(s)} = \frac{b_0 s^m + b_1 s^{m-1} + \cdots b_m}{s^n + a_1 s^{n-1} + \cdots a_n} = b_0 \frac{(s-z_1)(s-z_2)\ldots(s-z_m)}{(s-p_1)(s-p_2)\cdots(s-p_n)}.$$

The polynomial $a(s)$ has degree $n$ and the polynomial $b(s)$ has degree $m$. We assume that the integer $n_e = n - m$, which is called the *pole excess* is positive or zero. The controller is assumed to be a proportional controller with the transfer function $C(s) = k$. We will explore the poles of the closed loop system when the gain $k$ of the proportional controller changes.

The closed loop characteristic polynomial is

$$a_{cl} = a(s) + kb(s), \tag{11.13}$$

and the closed loop poles are the roots of $a_{cl}(s)$. The root-locus is a graph of the roots of $a_{cl}(s)$ as the gain $k$ is varied. Since the polynomial $a_{cl}(s)$ has degree $n$ the plot will have $n$ branches.

When the gain is $k$ zero we have $a_{cl}(s) = a(s)$ and the closed loop poles are equal to the open loop poles. To explore what happens for large gain make the following approximation for large $s$ and $k$

$$a_{cl}(s) = b(s)\Big(\frac{a(s)}{b(s)} + k\Big) \approx b(s)(s_e^n/b_0 + k). \tag{11.14}$$

For large $k$ the closed loop poles are approximately the roots of $b(s)$ and $\sqrt[n_e]{-b_0 k}$. A slightly better approximation is

$$s = x_0 + \sqrt[n_e]{-kb_0}, \qquad x_0 = \frac{1}{n_e}\left(\sum_{k=1}^{n} p_k - \sum_{k=1}^{m} z_k\right), \tag{11.15}$$

see Exercise 11.11. The asymptotes are thus $n_e$ lines that radiate from $s = x_0$. When $b_0 k > 0$ the lines have the angles $(\pi + 2l\pi)/n_e, l = 1, \cdots, n_e$ with the real line. Figure 11.13 shows the asymptotes of the root locus for large gain for different values of the pole excess $n_e$.

There are simple rules for sketching root loci. Let it suffice to mention three of them. The root locus has locally the symmetric star pattern at points where there are multiple roots, the number of branches depend on the multiplicity of the roots. For systems with $kb_0 > 0$ there are roots on segments of the real line where there are even numbers of poles and zeros to the right of the segment, see Exercise 11.12.

Figure 11.14 show root loci for systems with the transfer functions.

$$\begin{aligned} P_a(s) &= k\frac{s+1}{s^2}, \qquad P_b(s) &= k\frac{s+1}{s(s+2)(s^2+2s+4)} \\ P_c(s) &= k\frac{s+2}{s(s^2+1)}, \qquad P_d(s) &= k\frac{s^2+2s+2}{s(s^2+1)}. \end{aligned} \tag{11.16}$$

The locus in Figure 11.14a starts with two roots at the origin and the pattern is

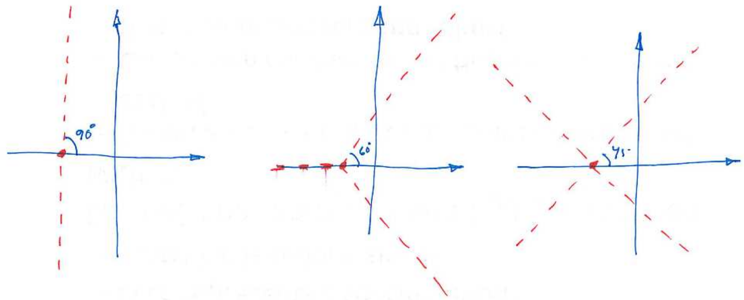


**Figure 11.13:** Asymptotes of of root locus for systems pole excess $n_e = 2$, 3 and 4. There are $n_e$ asymptotes radiate from the point given by equation 11.15

locally the has the star configuration. As the gain increases the locus bends towards because of the attraction of the zero, the locus is actually a circle around the zero. Two roots meet at the real axis, and there is the typical star pattern corrsponding to two roots. One root goes towards the zero and the other one goes to infinity along the negative real axis as the gain increases. It is easy to verify the locus on the real axis using the rule about loci on the real axis. Notice that stability improves when the controller gain is increased.

The locus in Figure 11.14b start at the open loop poles $s = -1, 0$ and $-1 \pm 3i$. The pole excess is $n_e = 3$ and the asymptotes which originate from $s = (0-2-2+1)/3 = -1$, have the corresponding pattern.

The locus in Figure 11.14c can be interpreted as the root locus for a PI control of a process with two complex poles at the imaginary axis. The asymptotes have the typical pattern for a system with pole excess $n_e = 2$. The asymptotes originate from $s = 2/2 = 1$. The root locus shows that the roots are in the right half plane for all gains.

The root locus is useful for qualitative arguments. For example, it follows from Figure Figure 11.13 that the closed loop system will always be unstable for suffi-

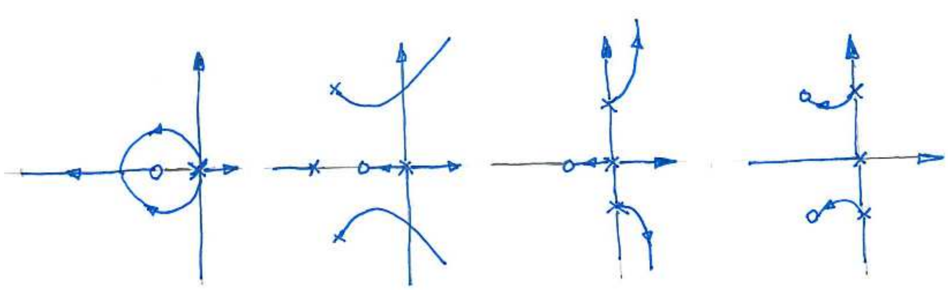

**Figure 11.14:** Examples of root loci for processes with the transfer functions given by equation (11.16).

ciently large gains if the pole excess is larger than $n_e = 2$ or if the process transfer function has zeros in the right half plane.

Consider a process with a right half plane zero at $s = 1$ and a right half plane pole at $s = 2$. This system cannot be stabilized by a controller which has all its poles and zeros in the left half plane. The loop transfer function $P(s)C(s)$ has the pole $s = 2$ and the zero $s = 1$ in the right half plane. It follows from the rule given above that he line segment $1 \le s \le 2$ is always part of the root locus and the closed loop system cannot be stable for any controller that has poles and zeros in the left half plane.

The rootlocus can also be used for design. Consider for example the system in Figure 11.14c which can represent PI control of a system with the transfer function

$$P(s) = \frac{1}{s^2+1}, \qquad C(s) = k\frac{s+2}{s}$$

The root locus in Figure 11.14c shows that the system is unstable for all values of the controller gain. To obtain a stable closed loop system we can attempt to choose a PID controller with zeros to the left of the undamped poles. The poles will attract the roots and we obtain the root locus shown in Figure 11.14d.

We have illustrated the root locus with a closed loop system with a proportional controller where the parameter is the gain. The root locus also be used to find the effects of other parameters as was illustrated in Example 4.15.

## 11.6 Fundamental Limitations

Although loop shaping gives us a great deal of flexibility in designing the closed loop response of a system, there are certain fundamental limits on what can be achieved. We consider here some of the primary performance limitations that can occur because of difficult dynamics; additional limitations related to robustness are considered in the next chapter.

### Right Half-Plane Poles and Zeros and Time Delays

There are linear systems that are inherently difficult to control. The limitations are related to poles and zeros in the right half-plane and time delays. To explore the limitations caused by poles and zeros in the right half-plane we factor the process transfer function as

$$P(s) = P_{mp}(s)P_{ap}(s), \tag{11.17}$$

where $P_{mp}$ is the minimum phase part and $P_{ap}$ is the nonminimum phase part. The factorization is normalized so that $|P_{ap}(i\omega)| = 1$, and the sign is chosen so that $P_{ap}$ has negative phase. The transfer function $P_{ap}$ is called an *all-pass system* because it has unit gain for all frequencies. Requiring that the phase margin be $\varphi_m$, we get

$$\arg L(i\omega_{gc}) = \arg P_{ap}(i\omega_{gc}) + \arg P_{mp}(i\omega_{gc}) + \arg C(i\omega_{gc}) \ge -\pi + \varphi_m, \tag{11.18}$$

where $C$ is the controller transfer function. Let $n_{gc}$ be the slope of the gain curve at the crossover frequency. Since $|P_{ap}(i\omega)| = 1$, it follows that

$$n_{gc} = \left.\frac{d\log|L(i\omega)|}{d\log\omega}\right|_{\omega=\omega_{gc}} = \left.\frac{d\log|P_{mp}(i\omega)C(i\omega)|}{d\log\omega}\right|_{\omega=\omega_{gc}}.$$

Assuming that the slope $n_{gc}$ is negative, it has to be larger than $-2$ for the system to be stable. It follows from Bode's relations, equation (9.8), that

$$\arg P_{mp}(i\omega) + \arg C(i\omega) \approx n_{gc}\frac{\pi}{2}.$$

Combining this with equation (11.18) gives the following inequality for the allowable phase lag of the all-pass part at the gain crossover frequency:

$$-\arg P_{ap}(i\omega_{gc}) \le \pi - \varphi_m + n_{gc}\frac{\pi}{2} =: \varphi_l. \tag{11.19}$$

This condition, which we call the *gain crossover frequency inequality*, shows that the gain crossover frequency must be chosen so that the phase lag of the nonminimum phase component is not too large. For systems with high robustness requirements we may choose a phase margin of 60° ($\varphi_m = \pi/3$) and a slope $n_{gc} = -1$, which gives an admissible phase lag $\varphi_l = \pi/6 = 0.52$ rad (30°). For systems where we can accept a lower robustness we may choose a phase margin of 45° ($\varphi_m = \pi/4$) and the slope $n_{gc} = -1/2$, which gives an admissible phase lag $\varphi_l = \pi/2 = 1.57$ rad (90°).

The crossover frequency inequality shows that nonminimum phase components impose severe restrictions on possible crossover frequencies. It also means that there are systems that cannot be controlled with sufficient stability margins. We illustrate the limitations in a number of commonly encountered situations.

**Example 11.7 Zero in the right half-plane**
The nonminimum phase part of the process transfer function for a system with a right half-plane zero is

$$P_{ap}(s) = \frac{z-s}{z+s},$$

where $z > 0$. The phase lag of the nonminimum phase part is

$$-\arg P_{ap}(i\omega) = 2\arctan\frac{\omega}{z}.$$

Since the phase lag of $P_{ap}$ increases with frequency, the inequality (11.19) gives the following bound on the crossover frequency:

$$\omega_{gc} < z\tan(\varphi_l/2). \tag{11.20}$$

With $\varphi_l = \pi/3$ we get $\omega_{gc} < 0.6z$. Slow right half-plane zeros ($z$ small) therefore give tighter restrictions on possible gain crossover frequencies than fast right half-plane zeros. ∇

Time delays also impose limitations similar to those given by zeros in the right half-plane. We can understand this intuitively from the Padé approximation

$$e^{-s\tau} \approx \frac{1-0.5s\tau}{1+0.5s\tau} = \frac{2/\tau - s}{2/\tau + s}.$$

A long time delay is thus equivalent to a slow right half-plane zero $z = 2/\tau$.

**Example 11.8 Pole in the right half-plane**
The nonminimum phase part of the transfer function for a system with a pole in the right half-plane is

$$P_{ap}(s) = \frac{s+p}{s-p},$$

where $p > 0$. The phase lag of the nonminimum phase part is

$$-\arg P_{ap}(i\omega) = 2\arctan\frac{p}{\omega},$$

and the crossover frequency inequality becomes

$$\omega_{\text{gc}} > \frac{p}{\tan(\varphi_l/2)}. \tag{11.21}$$

Right half-plane poles thus require that the closed loop system have a sufficiently high bandwidth. With $\varphi_l = \pi/3$ we get $\omega_{\text{gc}} > 1.7p$. Fast right half-plane poles ($p$ large) therefore give tighter restrictions on possible gain crossover frequencies than slow right half-plane poles. The control of unstable systems imposes minimum bandwidth requirements for process actuators and sensors. ∇

We will now consider systems with a right half-plane zero $z$ and a right half-plane pole $p$. If $p = z$, there will be an unstable subsystem that is neither reachable nor observable, and the system cannot be stabilized (see Section 7.5). We can therefore expect that the system is difficult to control if the right half-plane pole and zero are close. A straightforward way to use the crossover frequency inequality is to plot the phase of the nonminimum phase factor $P_{ap}$ of the process transfer function. Such a plot, which can be incorporated in an ordinary Bode plot, will immediately show the permissible gain crossover frequencies. An illustration is given in Figure 11.15, which shows the phase of $P_{ap}$ for systems with a right half-plane pole/zero pair and systems with a right half-plane pole and a time delay. If we require that the phase lag $\varphi_l$ of the nonminimum phase factor be less than 90°, we must require that the ratio $z/p$ be larger than 6 or smaller than 1/6 for systems with right half-plane poles and zeros and that the product $p\tau$ be less than 0.3 for systems with a time delay and a right half-plane pole. Notice the symmetry in the problem for $z > p$ and $z < p$: in either case the zeros and the poles must be sufficiently far apart (Exercise 11.14). Also notice that possible values of the gain crossover frequency $\omega_{\text{gc}}$ are quite restricted.

Using the theory of functions of complex variables, it can be shown that for systems with a right half-plane pole $p$ and a right half-plane zero $z$ (or a time delay

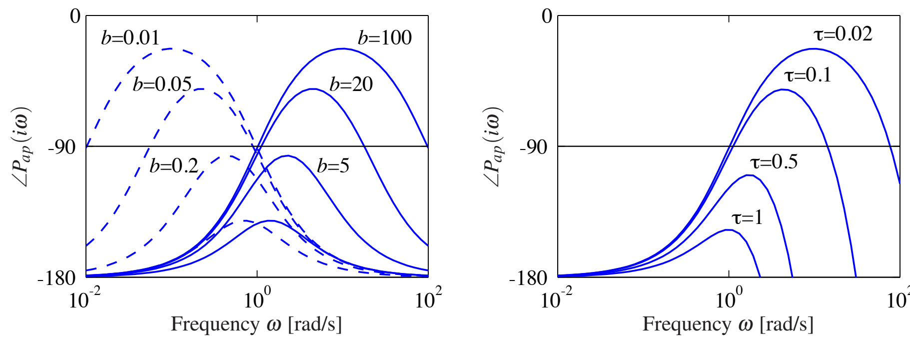


(a) RHP pole/zero pair

(b) RHP pole and time delay

**Figure 11.15:** Example limitations due to the gain crossover frequency inequality. The figures show the phase lag of the all-pass factor $P_{ap}$ as a function of frequency. Since the phase lag of $P_{ap}$ at the gain crossover frequency cannot be too large, it is necessary to choose the gain crossover frequency properly. All systems have a right half-plane pole at $s = 1$. The system in (a) has zeros at $s = 2$, 5, 20 and 100 (solid lines) and at $s = 0.5$, 0.2, 0.05 and 0.01 (dashed lines). The system in (b) has time delays $\tau = 0.02$ 0.1, 0.5 and 1.

$\tau$), any stabilizing controller gives sensitivity functions with the property

$$\sup_{\omega} |S(i\omega)| \geq \frac{p+z}{|p-z|}, \qquad \sup_{\omega} |T(i\omega)| \geq e^{p\tau}. \tag{11.22}$$

This result is proven in Exercise 11.15.

As the examples above show, right half-plane poles and zeros significantly limit the achievable performance of a system, hence one would like to avoid these whenever possible. The poles of a system depend on the intrinsic dynamics of the system and are given by the eigenvalues of the dynamics matrix $A$ of a linear system. Sensors and actuators have no effect on the poles; the only way to change poles is to redesign the system. Notice that this does not imply that unstable systems should be avoided. Unstable system may actually have advantages; one example is high-performance supersonic aircraft.

The zeros of a system depend on how the sensors and actuators are coupled to the states. The zeros depend on all the matrices $A$, $B$, $C$ and $D$ in a linear system. The zeros can thus be influenced by moving the sensors and actuators or by adding sensors and actuators. Notice that a fully actuated system $B = I$ does not have any zeros.

**Example 11.9 Balance system**

As an example of a system with both right half-plane poles and zeros, consider the balance system with zero damping, whose dynamics are given by

$$H_{\theta F} = \frac{ml}{-(M_tJ_t - m^2l^2)s^2 + mglM_t},$$
$$H_{pF} = \frac{-J_ts^2 + mgl}{s^2\big(-(M_tJ_t - m^2l^2)s^2 + mglM_t\big)}.$$

Assume that we want to stabilize the pendulum by using the cart position as the measured signal. The transfer function from the input force $F$ to the cart position $p$ has poles $\{0, 0, \pm\sqrt{mglM_t/(M_tJ_t - m^2l^2)}\}$ and zeros $\{\pm\sqrt{mgl/J_t}\}$. Using the parameters in Example 6.7, the right half-plane pole is at $p = 2.68$ and the zero is at $z = 2.09$. Equation (11.22) then gives $|S(i\omega)| \geq 8$, which shows that it is not possible to control the system robustly.

The right half-plane zero of the system can be eliminated by changing the output of the system. For example, if we choose the output to correspond to a position at a distance $r$ along the pendulum, we have $y = p - r\sin\theta$ and the transfer function for the linearized output becomes

$$H_{y,F} = H_{pF} - rH_{\theta F} = \frac{(mlr - J_t)s^2 + mgl}{s^2\big(-(M_tJ_t - m^2l^2)s^2 + mglM_t\big)}.$$

If we choose $r$ sufficiently large, then $mlr - J_t > 0$ and we eliminate the right half-plane zero, obtaining instead two pure imaginary zeros. The gain crossover frequency inequality is then based just on the right half-plane pole (Example 11.8). If our admissible phase lag for the nonminimum phase part is $\varphi_l = 45°$, then our gain crossover must satisfy

$$\omega_{\text{gc}} > \frac{p}{\tan(\varphi_l/2)} = 6.48 \text{ rad/s}.$$

If the actuators have sufficiently high bandwidth, e.g., a factor of 10 above $\omega_{\text{gc}}$ or roughly 10 Hz, then we can provide robust tracking up to this frequency. $\nabla$

### Bode's Integral Formula

In addition to providing adequate phase margin for robust stability, a typical control design will have to satisfy performance conditions on the sensitivity functions (Gang of Four). In particular, the sensitivity function $S = 1/(1+PC)$ represents the disturbance attenuation and also relates the tracking error $e$ to the reference signal: we usually want the sensitivity to be small over the range of frequencies where we want small tracking error and good disturbance attenuation. A basic problem is to investigate if $S$ can be made small over a large frequency range. We will start by investigating an example.

**Example 11.10 System that admits small sensitivities**
Consider a closed loop system consisting of a first-order process and a proportional

controller. Let the loop transfer function be

$$L(s) = PC = \frac{k}{s+1},$$

where parameter $k$ is the controller gain. The sensitivity function is

$$S(s) = \frac{s+1}{s+1+k}$$

and we have

$$|S(i\omega)| = \sqrt{\frac{1+\omega^2}{1+2k+k^2+\omega^2}}.$$

This implies that $|S(i\omega)| < 1$ for all finite frequencies and that the sensitivity can be made arbitrarily small for any finite frequency by making $k$ sufficiently large. ∇

The system in Example 11.10 is unfortunately an exception. The key feature of the system is that the Nyquist curve of the process is completely contained in the right half-plane. Such systems are called *passive*, and their transfer functions are *positive real*. For typical control systems there are severe constraints on the sensitivity function. The following theorem, due to Bode, provides insights into the limits of performance under feedback.

**Theorem 11.1** (Bode's integral formula)**.** *Assume that the loop transfer function $L(s)$ of a feedback system goes to zero faster than $1/s$ as $s \to \infty$, and let $S(s)$ be the sensitivity function. If the loop transfer function has poles $p_k$ in the right half-plane, then the sensitivity function satisfies the following integral:*

$$\int_0^\infty \log|S(i\omega)|\,d\omega = \int_0^\infty \log\frac{1}{|1+L(i\omega)|}\,d\omega = \pi\sum p_k. \qquad (11.23)$$

Equation (11.23) implies that there are fundamental limitations to what can be achieved by control and that control design can be viewed as a redistribution of disturbance attenuation over different frequencies. In particular, this equation shows that if the sensitivity function is made smaller for some frequencies, it must increase at other frequencies so that the integral of $\log|S(i\omega)|$ remains constant. This means that if disturbance attenuation is improved in one frequency range, it will be worse in another, a property sometime referred to as the *waterbed effect*. It also follows that systems with open loop poles in the right half-plane have larger overall sensitivity than stable systems.

Equation (11.23) can be regarded as a *conservation law*: if the loop transfer function has no poles in the right half-plane, the equation simplifies to

$$\int_0^\infty \log|S(i\omega)|d\omega = 0.$$

This formula can be given a nice geometric interpretation as illustrated in Figure 11.16, which shows $\log|S(i\omega)|$ as a function of $\omega$. The area over the horizontal axis must be equal to the area under the axis when the frequency is plotted on a *linear* scale. Thus if we wish to make the sensitivity smaller up to some frequency

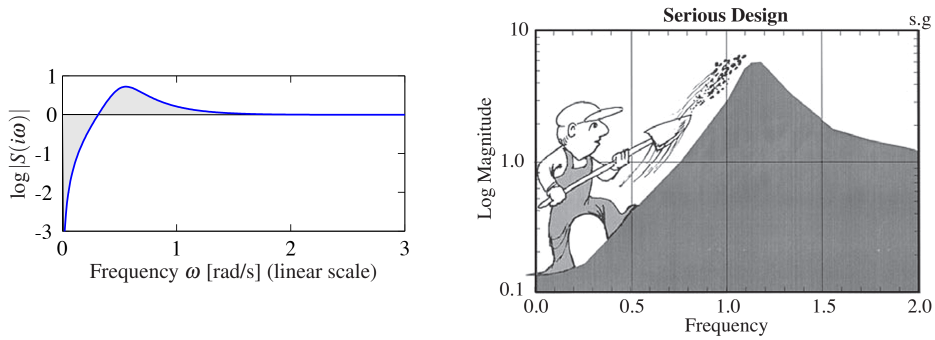


(a) Bode integral formula (b) Control design process

**Figure 11.16:** Interpretation of the *waterbed effect*. The function $\log|S(i\omega)|$ is plotted versus $\omega$ in linear scales in (a). According to Bode's integral formula (11.23), the area of $\log|S(i\omega)|$ above zero must be equal to the area below zero. Gunter Stein's interpretation of design as a trade-off of sensitivities at different frequencies is shown in (b) (from [Ste03]).

$\omega_{sc}$, we must balance this by increased sensitivity above $\omega_{sc}$. Control system design can be viewed as trading the disturbance attenuation at some frequencies for disturbance amplification at other frequencies. Notice that the system in Example 11.10 violates the condition that $\lim_{s\to\infty} sL(s) = 0$ and hence the integral formula does not apply.

There is result analogous to equation (11.23) for the complementary sensitivity function:

$$\int_0^\infty \frac{\log|T(i\omega)|}{\omega^2}\,d\omega = \pi \sum \frac{1}{z_i}, \tag{11.24}$$

where the summation is over all right half-plane zeros. Notice that slow right half-plane zeros are worse than fast ones and that fast right half-plane poles are worse than slow ones.

**Example 11.11 X-29 aircraft**

As an example of the application of Bode's integral formula, we present an analysis of the control system for the X-29 aircraft (see Figure 11.17a), which has an unusual configuration of aerodynamic surfaces that are designed to enhance its maneuverability. This analysis was originally carried out by Gunter Stein in his article "Respect the Unstable" [Ste03], which is also the source of the quote at the beginning of this chapter.

To analyze this system, we make use of a small set of parameters that describe the key properties of the system. The X-29 has longitudinal dynamics that are very similar to inverted pendulum dynamics (Exercise 8.3) and, in particular, have a pair of poles at approximately $p = \pm 6$ and a zero at $z = 26$. The actuators that stabilize the pitch have a bandwidth of $\omega_a = 40$ rad/s and the desired bandwidth of the pitch control loop is $\omega_1 = 3$ rad/s. Since the ratio of the zero to the pole is only 4.3, we may expect that it may be difficult to achieve the specifications.

To evaluate the achievable performance, we search for a control law such that

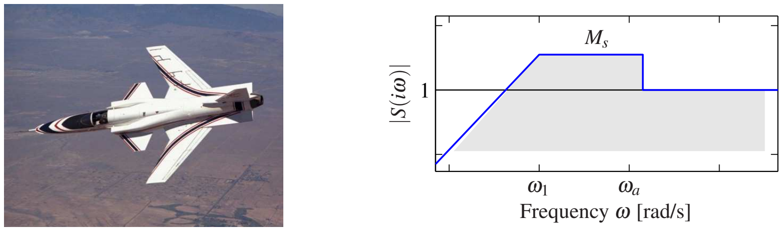


(a) X-29 aircraft (b) Sensitivity analysis

**Figure 11.17:** X-29 flight control system. The aircraft makes use of forward swept wings and a set of canards on the fuselage to achieve high maneuverability (a). The desired sensitivity for the closed loop system is shown in (b). We seek to use our control authority to shape the sensitivity curve so that we have low sensitivity (good performance) up to frequency $\omega_1$ by creating higher sensitivity up to our actuator bandwidth $\omega_a$.

the sensitivity function is small up to the desired bandwidth and not greater than $M_s$ beyond that frequency. Because of the Bode integral formula, we know that $M_s$ must be greater than 1 at high frequencies to balance the small sensitivity at low frequency. We thus ask if we can find a controller that has the shape shown in Figure 11.17b with the smallest value of $M_s$. Note that the sensitivity above the frequency $\omega_a$ is not specified since we have no actuator authority at that frequency. However, assuming that the process dynamics fall off at high frequency, the sensitivity at high frequency will approach 1. Thus, we desire to design a closed loop system that has low sensitivity at frequencies below $\omega_1$ and sensitivity that is not too large between $\omega_1$ and $\omega_a$.

From Bode's integral formula, we know that whatever controller we choose, equation (11.23) must hold. We will assume that the sensitivity function is given by

$$|S(i\omega)| = \begin{cases} \frac{\omega M_s}{\omega_1} & \omega \le \omega_1 \\ M_s & \omega_1 \le \omega \le \omega_a, \end{cases}$$

corresponding to Figure 11.17b. If we further assume that $|L(s)| \le \delta/\omega^2$ for frequencies larger than the actuator bandwidth, Bode's integral becomes

$$\begin{aligned} \int_0^\infty \log|S(i\omega)|\,d\omega &= \int_0^{\omega_a} \log|S(i\omega)|\,d\omega \\ &= \int_0^{\omega_1} \log\frac{\omega M_s}{\omega_1}\,d\omega + (\omega_a - \omega_1)\log M_s = \pi p. \end{aligned}$$

Evaluation of the integral gives $-\omega_1 + \omega_a \log M_s = \pi p$ or

$$M_s = e^{(\pi p + \omega_1)/\omega_a}.$$

This formula tells us what the achievable value of $M_s$ will be for the given control specifications. In particular, using $p = 6$, $\omega_1 = 3$ and $\omega_a = 40$ rad/s, we find that $M_s = 1.75$, which means that in the range of frequencies between $\omega_1$ and $\omega_a$, disturbances at the input to the process dynamics (such as wind) will be amplified

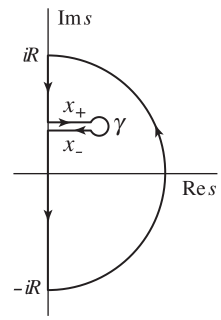


**Figure 11.18:** Contour used to prove Bode's theorem. For each right half-plane pole we create a path from the imaginary axis that encircles the pole as shown. To avoid clutter we have shown only one of the paths that enclose one right half-plane.

by a factor of 1.75 in terms of their effect on the aircraft.

Another way to view these results is to compute the phase margin that corresponds to the given level of sensitivity. Since the peak sensitivity normally occurs at or near the crossover frequency, we can compute the phase margin corresponding to $M_s = 1.75$. As shown in Exercise 11.16, the maximum achievable phase margin for this system is approximately 35°, which is below the usual design limit of 45° in aerospace systems. The zero at $s = 26$ limits the maximum gain crossover that can be achieved. ∇

### Derivation of Bode's Formula

We now derive Bode's integral formula (Theorem 11.1). This is a technical section that requires some knowledge of the theory of complex variables, in particular contour integration. Assume that the loop transfer function has distinct poles at $s = p_k$ in the right half-plane and that $L(s)$ goes to zero faster than $1/s$ for large values of $s$.

Consider the integral of the logarithm of the sensitivity function $S(s) = 1/(1+L(s))$ over the contour shown in Figure 11.18. The contour encloses the right half-plane except for the points $s = p_k$ where the loop transfer function $L(s) = P(s)C(s)$ has poles and the sensitivity function $S(s)$ has zeros. The direction of the contour is counterclockwise.

The integral of the log of the sensitivity function around this contour is given by

$$\int_\Gamma \log(S(s))\,ds = \int_{iR}^{-iR} \log(S(s))\,ds + \int_R \log(S(s))\,ds + \sum_k \int_\gamma \log(S(s))\,ds$$
$$= I_1 + I_2 + I_3 = 0,$$

where $R$ is a large semicircle on the right and $\gamma_k$ is the contour starting on the imaginary axis at $s = \operatorname{Im} p_k$ and a small circle enclosing the pole $p_k$. The integral is zero because the function $\log S(s)$ is analytic inside the contour. We have

$$I_1 = -i\int_{-R}^{R} \log(S(i\omega))d\omega = -2i\int_0^R \log(|S(i\omega)|)d\omega$$

because the real part of $\log S(i\omega)$ is an even function and the imaginary part is an odd function. Furthermore we have

$$I_2 = \int_R \log(S(s))\, ds = -\int_R \log(1+L(s))\, ds \approx -\int_R L(s)\, ds.$$

Since $L(s)$ goes to zero faster than $1/s$ for large $s$, the integral goes to zero when the radius of the circle goes to infinity.

Next we consider the integral $I_3$. For this purpose we split the contour into three parts $X_+$, $\gamma$ and $X_-$, as indicated in Figure 11.18. We can then write the integral as

$$I_3 = \int_{X_+} \log S(s)\, ds + \int_\gamma \log S(s)\, ds + \int_{X-} \log S(s)\, ds.$$

The contour $\gamma$ is a small circle with radius $r$ around the pole $p_k$. The magnitude of the integrand is of the order $\log r$, and the length of the path is $2\pi r$. The integral thus goes to zero as the radius $r$ goes to zero. Since $S(s) \approx k/(s-p_k)$ close to the pole, the argument of $S(s)$ decreases by $2\pi$ as the contour encircles the pole. On the contours $X_+$ and $X_-$ we therefore have

$$|S_{X_+}| = |S_{X_-}|, \qquad \arg S_{X_-} = \arg S_{X_+} - 2\pi.$$

Hence

$$\log(S_{X_+}) - \log(S_{X_-}) = 2\pi i,$$

and we get

$$\int_{X_+} \log S(s)\, ds + \int_{X_-} \log S(s)\, ds = 2\pi\; i \operatorname{Re} p_k.$$

Repeating the argument for all poles $p_k$ in the right half plane, letting the small circles go to zero and the large circle go to infinity gives

$$I_1 + I_2 + I_3 = -2i\int_0^R \log|S(i\omega)|d\omega + i\sum_k 2\pi \operatorname{Re} p_k = 0.$$

Since complex poles appear as complex conjugate pairs, $\sum_k \operatorname{Re} p_k = \sum_k p_k$, which gives Bode's formula (11.23).

## 11.7 Design Example

In this section we present a detailed example that illustrates the main design techniques described in this chapter.

**Example 11.12 Lateral control of a vectored thrust aircraft**
The problem of controlling the motion of a vertical takeoff and landing (VTOL) aircraft was introduced in Example 2.10 and in Example 11.6, where we designed

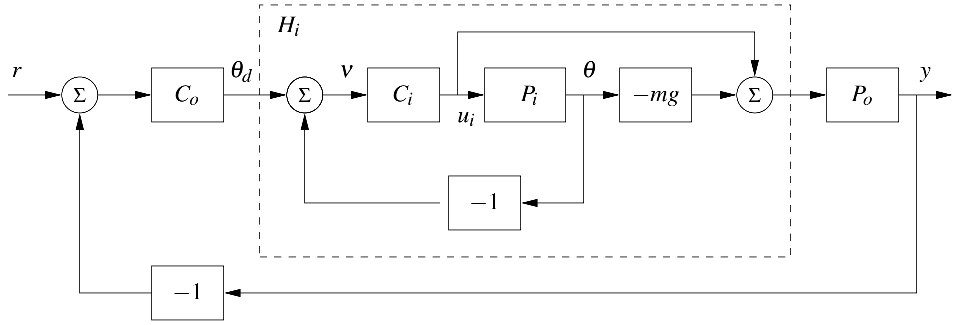


**Figure 11.19:** Inner/outer control design for a vectored thrust aircraft. The inner loop $H_i$ controls the roll angle of the aircraft using the vectored thrust. The outer loop controller $C_o$ commands the roll angle to regulate the lateral position. The process dynamics are decomposed into inner loop ($P_i$) and outer loop ($P_o$) dynamics, which combine to form the full dynamics for the aircraft.

.

a controller for the roll dynamics. We now wish to control the position of the aircraft, a problem that requires stabilization of both the attitude and the position.

To control the lateral dynamics of the vectored thrust aircraft, we make use of a "inner/outer" loop design methodology, as illustrated in Figure 11.19. This diagram shows the process dynamics and controller divided into two components: an *inner loop* consisting of the roll dynamics and control and an *outer loop* consisting of the lateral position dynamics and controller. This decomposition follows the block diagram representation of the dynamics given in Exercise 8.10.

The approach that we take is to design a controller $C_i$ for the inner loop so that the resulting closed loop system $H_i$ provides fast and accurate control of the roll angle for the aircraft. We then design a controller for the lateral position that uses the approximation that we can directly control the roll angle as an input to the dynamics controlling the position. Under the assumption that the dynamics of the roll controller are fast relative to the desired bandwidth of the lateral position control, we can then combine the inner and outer loop controllers to get a single controller for the entire system. As a performance specification for the entire system, we would like to have zero steady-state error in the lateral position, a bandwidth of approximately 1 rad/s and a phase margin of 45°.

For the inner loop, we choose our design specification to provide the outer loop with accurate and fast control of the roll. The inner loop dynamics are given by

$$P_i = H_{\theta u_1} = \frac{r}{Js^2}.$$

We choose the desired bandwidth to be 10 rad/s (10 times that of the outer loop) and the low-frequency error to be no more than 5%. This specification is satisfied using the lead compensator of Example 11.6 designed previously, so we choose

$$C_i(s) = k\frac{s+a}{s+b}, \qquad a = 2, \quad b = 50, \quad k = 1.$$

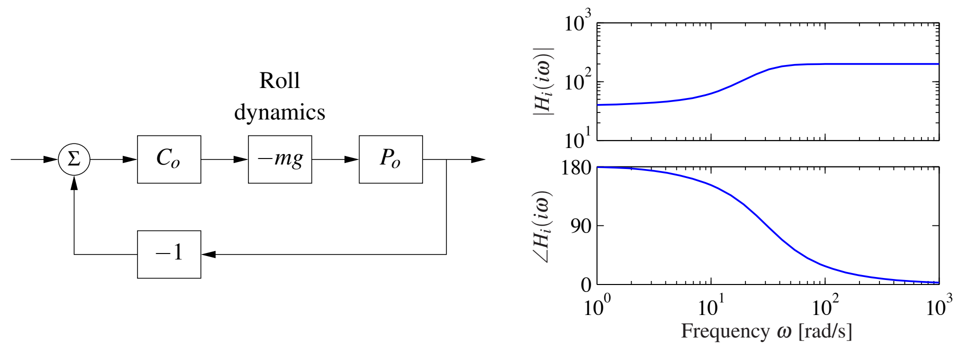


(a) Outer loop approximation (b) Actual roll dynamics

**Figure 11.20:** Outer loop control design for a vectored thrust aircraft. (a) The outer loop approximates the roll dynamics as a state gain $-mg$. (b) The Bode plot for the roll dynamics, indicating that this approximation is accurate up to approximately 10 rad/s.

The closed loop dynamics for the system satisfy

$$H_i = \frac{C_i}{1+C_iP_i} - mg\frac{C_iP_i}{1+C_iP_i} = \frac{C_i(1-mgP_i)}{1+C_iP_i}.$$

A plot of the magnitude of this transfer function is shown in Figure 11.20, and we see that $H_i \approx -mg = -39.2$ is a good approximation up to 10 rad/s.

To design the outer loop controller, we assume the inner loop roll control is perfect, so that we can take $\theta_d$ as the input to our lateral dynamics. Following the diagram shown in Exercise 8.10, the outer loop dynamics can be written as

$$P(s) = H_i(0)P_o(s) = \frac{H_i(0)}{ms^2+cs},$$

where we replace $H_i(s)$ with $H_i(0)$ to reflect our approximation that the inner loop will eventually track our commanded input. Of course, this approximation may not be valid, and so we must verify this when we complete our design.

Our control goal is now to design a controller that gives zero steady-state error in $y$ and has a bandwidth of 1 rad/s. The outer loop process dynamics are given by a second-order integrator, and we can again use a simple lead compensator to satisfy the specifications. We also choose the design such that the loop transfer function for the outer loop has $|L_o| < 0.1$ for $\omega > 10$ rad/s, so that the $H_i$ dynamics can be neglected. We choose the controller to be of the form

$$C_o(s) = -k_o\frac{s+a_o}{s+b_o},$$

with the negative sign to cancel the negative sign in the process dynamics. To find the location of the poles, we note that the phase lead flattens out at approximately $b_o/10$. We desire phase lead at crossover, and we desire the crossover at $\omega_{\text{gc}} =$ 1 rad/s, so this gives $b_o = 10$. To ensure that we have adequate phase lead, we must choose $a_o$ such that $b_o/10 < 10a_o < b_o$, which implies that $a_o$ should be between

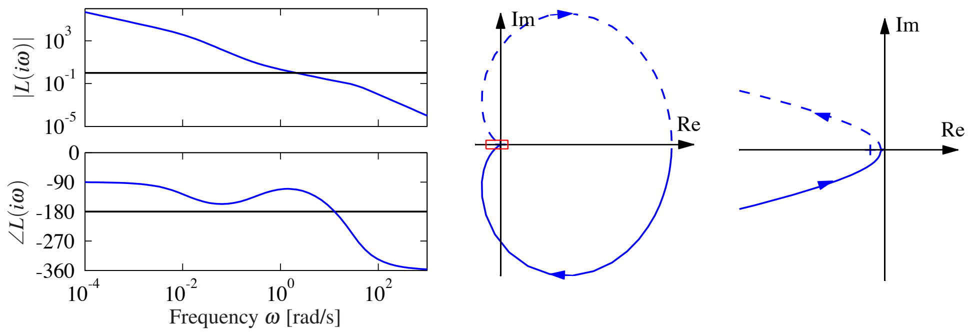


(a) Bode plot (b) Nyquist plot

**Figure 11.21:** Inner/outer loop controller for a vectored thrust aircraft. The Bode plot (a) and Nyquist plot (b) for the transfer function for the combined inner and outer loop transfer functions are shown. The system has a phase margin of 68° and a gain margin of 6.2.

0.1 and 1. We choose $a_o = 0.3$. Finally, we need to set the gain of the system such that at crossover the loop gain has magnitude 1. A simple calculation shows that $k_o = 2$ satisfies this objective. Thus, the final outer loop controller becomes

$$C_o(s) = -2\frac{s+0.3}{s+10}.$$

Finally, we can combine the inner and outer loop controllers and verify that the system has the desired closed loop performance. The Bode and Nyquist plots corresponding to Figure 11.19 with inner and outer loop controllers are shown in Figure 11.21, and we see that the specifications are satisfied. In addition, we show the Gang of Four in Figure 11.22, and we see that the transfer functions between all inputs and outputs are reasonable. The sensitivity to load disturbances $PS$ is large at low frequency because the controller does not have integral action.

The approach of splitting the dynamics into an inner and an outer loop is common in many control applications and can lead to simpler designs for complex systems. Indeed, for the aircraft dynamics studied in this example, it is very challenging to directly design a controller from the lateral position $x$ to the input $u_1$. The use of the additional measurement of $\theta$ greatly simplifies the design because it can be broken up into simpler pieces. ∇

## 11.8 Further Reading

Design by loop shaping was a key element in the early development of control, and systematic design methods were developed; see James, Nichols and Phillips [JNP47], Chestnut and Mayer [CM51], Truxal [Tru55] and Thaler [Tha89]. Loop shaping is also treated in standard textbooks such as Franklin, Powell and Emami-Naeini [FPEN05], Dorf and Bishop [DB04], Kuo and Golnaraghi [KG02] and Ogata [Oga01]. Systems with two degrees of freedom were developed by Horowitz [Hor63],

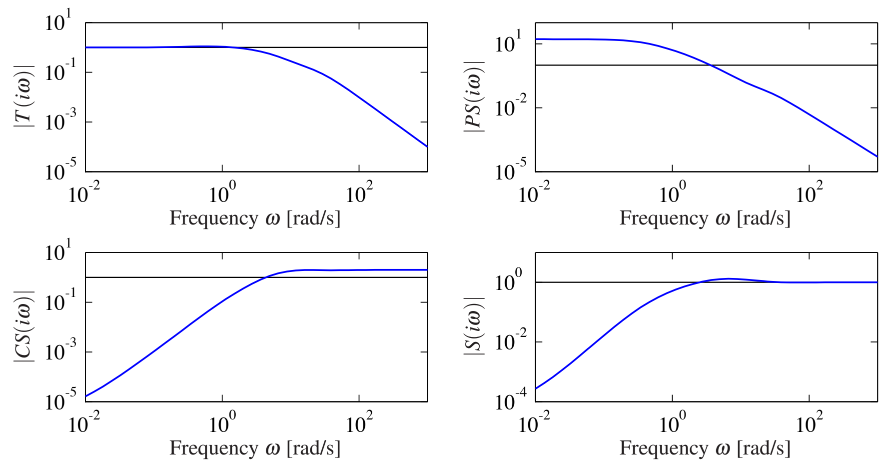


**Figure 11.22:** Gang of Four for vectored thrust aircraft system.

who also discussed the limitations of poles and zeros in the right half-plane. Fundamental results on limitations are given in Bode [Bod45]; more recent presentations are found in Goodwin, Graebe and Salgado [GGS01]. The treatment in Section 11.6 is based on [Åst00]. Much of the early work was based on the loop transfer function; the importance of the sensitivity functions appeared in connection with the development in the 1980s that resulted in $H_\infty$ design methods. A compact presentation is given in the texts by Doyle, Francis and Tannenbaum [DFT92] and Zhou, Doyle and Glover [ZDG96]. Loop shaping was integrated with the robust control theory in McFarlane and Glover [MG90] and Vinnicombe [Vin01]. Comprehensive treatments of control system design are given in Maciejowski [Mac89] and Goodwin, Graebe and Salgado [GGS01].

## Exercises

**11.1** Consider the system in Figure 11.1. Give all signal pairs that are related by the transfer functions $1/(1+PC)$, $P/(1+PC)$, $C/(1+PC)$ and $PC/(1+PC)$.

**11.2** Consider the system in Example 11.1. Choose the parameters $a = -1$ and compute the time and frequency responses for all the transfer functions in the Gang of Four for controllers with $k = 0.2$ and $k = 5$.

**11.3** (Equivalence of Figures 11.1 and 11.2) Consider the system in Figure 11.1 and let the outputs of interest be $z = (\eta, \nu)$ and the major disturbances be $w = (n, d)$. Show that the system can be represented by Figure 11.2 and give the matrix transfer functions $\mathscr{P}$ and $\mathscr{C}$. Verify that the elements of the closed loop transfer function $H_{zw}$ are the Gang of Four.

**11.4** Consider the spring–mass system given by (2.14), which has the transfer function

$$P(s) = \frac{1}{ms^2 + cs + k}.$$

Design a feedforward compensator that gives a response with critical damping ($\zeta = 1$).

**11.5** (Sensitivity of feedback and feedforward) Consider the system in Figure 11.1 and let $G_{yr}$ be the transfer function relating the measured signal $y$ to the reference $r$. Show that the sensitivities of $G_{yr}$ with respect to the feedforward and feedback transfer functions $F$ and $C$ are given by $dG_{yr}/dF = CP/(1+PC)$ and $dG_{yr}/dC = FP/(1+PC)^2 = G_{yr}S/C$.

**11.6** (Equivalence of controllers with two degrees of freedom) Show that the systems in Figures 11.1 and 11.3 give the same responses to command signals if $F_mC + F_u = CF$.

**11.7** (Disturbance attenuation) Consider the feedback system shown in Figure 11.1. Assume that the reference signal is constant. Let $y_{ol}$ be the measured output when there is no feedback and $y_{cl}$ be the output with feedback. Show that $Y_{cl}(s) = S(s)Y_{ol}(s)$, where $S$ is the sensitivity function.

**11.8** (Disturbance reduction through feedback) Consider a problem in which an output variable has been measured to estimate the potential for disturbance attenuation by feedback. Suppose an analysis shows that it is possible to design a closed loop system with the sensitivity function

$$S(s) = \frac{s}{s^2 + s + 1}.$$

Estimate the possible disturbance reduction when the measured disturbance is

$$y(t) = 5\sin(0.1t) + 3\sin(0.17t) + 0.5\cos(0.9t) + 0.1t.$$

**11.9** Show that the effect of high frequency measurement noise on the control signal for the system in Example 11.4 can be approximated by

$$CS \approx C = \frac{k_d s}{(sT_f)^2/2 + sT_f + 1},$$

and that the largest value of $|CS(i\omega)|$ is $k_d/T_f$ which occurs for $\omega = \sqrt{2}/T_f$.

**11.10** (Attenuation of low-frequency sinusoidal disturbances) Integral action eliminates constant disturbances and reduces low-frequency disturbances because the controller gain is infinite at zero frequency. A similar idea can be used to reduce the effects of sinusoidal disturbances of known frequency $\omega_0$ by using the controller

$$C(s) = k_p + \frac{k_s s}{s^2 + 2\zeta\omega_0 s + \omega_0^2}.$$

This controller has the gain $C_s(i\omega_0) = k_p + k_s/(2\zeta)$ for the frequency $\omega_0$, which can be large by choosing a small value of $\zeta$. Assume that the process has the transfer function $P(s) = 1/s$. Determine the Bode plot of the loop transfer function and simulate the system. Compare the results with PI control.

**11.11** (Asymptotes of root locus) Consider proportional control of a system with the transfer function

$$P(s) = \frac{b(s)}{a(s)} = \frac{b_0 s^m + b_1 s^{m-1} + \cdots b_m}{s^n + a_1 s^{n-1} + \cdots a_n} = b_0 \frac{(s-z_1)(s-z_2)\ldots(s-z_m)}{(s-p_1)(s-p_2)\cdots(s-p_n)}.$$

Show that the root locus has asymptotes that are straight line that emerge from the point

$$s = \frac{1}{n_e}\Big(\sum_{k=1}^{n} p_k - \sum_{k=1}^{m} z_k\Big),$$

where $n_e$ is the pole excess of the transfer function.

**11.12** (Real line segments of root locus) Consider proportional control a process with a rational transfer function. Assume that $b_o k > 0$, show that the root locus has segments on the real line there are an odd number of real poles and zeros to the right the segment.

**11.13** Consider a lead compensator with the transfer function

$$C_n(s) = \Big(\frac{s\sqrt[n]{k} + a}{s+a}\Big)^n,$$

which has zero frequency gain $C(0) = 1$ and high-frequency gain $C(\infty) = k$. Show that the gain required to give a given phase lead $\varphi$ is

$$k = \Big(1 + 2\tan^2(\varphi/n) + 2\tan(\varphi/n)\sqrt{1+\tan^2(\varphi/n)}\Big)^n,$$

and that $\lim_{n\to\infty} k = e^{2\varphi}$.

**11.14** Consider a process with the loop transfer function

$$L(s) = k\frac{z-s}{s-p},$$

with positive $z$ and $p$. Show that the system is stable if $p/z < k < 1$ or $1 < k < p/z$, and that the largest stability margin is $s_m = |p-z|/(p+z)$ is obtained for $k = 2p/(p+z)$. Determine the pole/zero ratios that gives the stability margin $s_m = 2/3$.

**11.15** Prove the inequalities given by equation (11.22). (Hint: Use the maximum modulus theorem.)

**11.16** (Phase margin formulas) Show that the relationship between the phase margin and the values of the sensitivity functions at gain crossover is given by

$$|S(i\omega_{gc})| = |T(i\omega_{gc})| = \frac{1}{2\sin(\varphi_m/2)}.$$

**11.17** (Stabilization of an inverted pendulum with visual feedback) Consider stabilization of an inverted pendulum based on visual feedback using a video camera with a 50-Hz frame rate. Let the effective pendulum length be $l$. Assume that we want the loop transfer function to have a slope of $n_{gc} = -1/2$ at the crossover frequency. Use the gain crossover frequency inequality to determine the minimum length of the pendulum that can be stabilized if we desire a phase margin of 45°.

**11.18** (Rear-steered bicycle) Consider the simple model of a bicycle in Equation (A.5), which has one pole in the right half-plane. The model is also valid for a bicycle with rear wheel steering, but the sign of the velocity is then reversed and the system also has a zero in the right half-plane. Use the results of Exercise 11.14 to give a condition on the physical parameters that admits a controller with the stability margin $s_m$.

**11.19** Prove the formula (11.24) for the complementary sensitivity.